Indian Journal of Chemical Technology
Vol. 31, November 2024, pp. 879-888
DOI: 10.56042/ijct.v31i6.11340

Bio-oil production: A comparative analysis of catalytic pyrolysis with cobalt catalyst versus direct pyrolysis of Azolla and Ulva biomasses

S. Pourkarimi[1]*, M. Saberdelsadeh[2], H. Nouri[3] & A. Hallajisani[1]

[1]Biofuel laboratory, Caspian Faculty of Engineering, College of Engineering, University of Tehran, Iran, P.O. BOX 111454653, Iran

[2]Faculty of Engineering University of Porto, 4200-465 Porto, Portugal

[3]Chemical and Biological Engineering Department, Iowa State University, Ames, Iowa, USA

*E-mail: sara.pourkarimi@phd.iaurasht.ac.ir

Received 23 May 2024; accepted 18 September 2024

Bio-oil is a key alternative to fossil fuels, and its commercialization requires assessing production quality and quantity. Catalysts play a crucial role in the bio-oil production process. This study evaluates the impact of cobalt-based zeolite (Co/HZSM-5) catalysts on the pyrolysis of Azolla and Ulva biomasses, focusing on bio-oil production and comparing it with direct pyrolysis. It demonstrated that catalytic pyrolysis improved the high heat value (HHV) and energy yield of the bio-oil compared with direct pyrolysis.Specifically, for Azolla, the bio-oil yield decreased from 30.64% in direct pyrolysis to 23.5% with the catalyst, while HHV increased from 28.6 MJ/kg to 33.2 MJ/kg. For Ulva, bio-oil yield fell from 34.43% to 26.1%, with HHV rising from 30.7 MJ/kg to 32.26 MJ/kg. Catalytic pyrolysis also enhanced energy recovery, achieving 48.37% for Azolla and 69.02% for Ulva. The process altered the distribution of pyrolysis products: biogas yield dropped from 37% to 27.14% for Azolla and from 30.5% to 16.57% for Ulva, while biochar yield increased from 39.5% to 42.21% for Azolla and from 43.4% to 49% for Ulva. These results suggest that catalytic pyrolysis is effective in producing higher quality bio-oil and improves overall energy efficiency.

Keywords: Azolla biomass, Bio-oil, Catalytic pyrolysis, Cobalt Catalyst, HHV, Ulva biomass

Introduction

As fossil fuels cannot be sustained and have negative ecological consequences, green and sustainable alternatives to energy must be explored. A sustainable energy source that is gaining a lot of attention is biomass[1,2]. A clean and renewable energy source obtained by burning different biofuels such as biodiesel, biogas, bioethanol, and bio-oil is bioenergy. These fuels are obtained from different bio sources like oil seeds, agricultural wastes, animal fat, microorganisms, aquatic plants (e.g. algae, ferns), urban wastes, sludges from wastewater treatment sites, and organic wastes (e.g. plastics) [3–6].

Azolla and Ulva are two types of aquatic biomasses with significant potential for bioenergy production. Azolla, a fern, is known for its rapid growth and high nitrogen content, making it a promising candidate for bioenergy applications. It is predominantly found in subtropical regions and can be cultivated in diverse aquatic environments. Azolla's high protein content and high growth rate contribute to its potential as a biomass feedstock for bio-oil production.Ulva, commonly known as green seaweed, is widely distributed along coastlines and has a high carbohydrate content. The plant grows quickly and is abundant in marine environments, making it an accessible and renewable source of bioenergy. The high cellulose content in Ulva makes it a viable candidate for conversion into bio-oil through pyrolysis[7].

Among the biofuels, bio-oil (products of thermal cracking of biomasses through a process called pyrolysis) does not need downstream processes, which makes it a promising choice. Along with a variety of parameters like the type of biomass, heating rate, temperature, and rest time that affect the process of pyrolysis of biomass, using catalyzers (given the type and volume of catalyst) can be a key qualitative and quantitative factor in producing biofuel[8,9]. Based on this, pyrolysis process can be catalytic or direct pyrolysis[10,11]. The bio-oil of catalytic pyrolysis has a better carbon content and a lower oxygen, which increases its heat value and quality[12,13].

The recommended mechanism for catalytic pyrolysis is a combination of free radicals and carbonium ion mechanism (based on Bronsted-Lowry acid-based theory)[14]. The catalysts used in the process

mostly contain metal compounds like metal oxides. In many cases, catalysts are comprised of two sections (base and booster), which improve the process yield. One of the main compounds used in pyrolysis process, which is used as the base, is zeolite [15,16]. Zeolite has a 3D, latticed, and pentagon molecular structure that is formed by alumina and silica at different ratios. Studies have listed a wide range of usage of zeolite to convert different biomasses such as cellulose, lignin, and algae biomasses into bio-oil through pyrolysis process [17].

Jones et al. (2009) examined the production of bio-oil using cellulose and lignin biomasses and zeolite catalysts. They reported that the catalyst deoxygenates the biomasses in the first phase and then facilitates hydrocarbons conversion of higher heat value [18]. The role of zeolite-based materials in biomass catalytic deoxygenation is explained in the review[19].

Amalina et al. (2023) examined the microwave-assisted pyrolysis (MAP) of biomass has shown satisfactory generating high-quality bio-oils[20]. Pan et al. (2010) examined the role of catalyst ratio to feed and temperature effect for *Nannochloropsis sp.* microalgae catalytic pyrolysis using HZSM-5 catalyst (Si/Al=25). The ratio of feed to catalyst was equal to 1/20% (w/w) and the operation temperature was 300-500°C. Eventually, the top bio-oil yield was realized with ratio of catalyst to feed equal to 20% (w/w) and operation temperature equal to 400°C, which was about 25%. Moreover, oxygen production was decreased by the catalyst from 30.1% to 19.5% and increased value of heat from 24.6 MJ/kg to 32.7 MJ/kg [21]. Mohamed et al. (2017) conducted a study on using different ratios of alumina-based cobalt to feed (5-25%) to covert fruit tree wastes into bio-oil using catalytic pyrolysis. They demonstrated that increasing the ratio of cobalt in the catalyst increased the yield of bio-oil and decreased coke.In addition, the highest bio-oil yield was equal to 41.89% with alumina-based cobalt ratio of 20% [22]. Ma et al. (2019) studied using zeolite catalyst ZSM-5 with ratio to feed in 2-10% range for bio-oil production from Ulva microalgae at 400°C. They showed that the top bio-oil yield was 41.3% with catalyst/feed ratio of 10% [23]. Chen et al. (2021) examined bio-oil production using sawdust and corn waste pyrolysis at operational temperature of 500°C. They used different HZSM-5/feed ratios (1:1, 1:5, and 1:10). As shown by the result, the top bio-oil yield was 6% using sawdust with catalyst/feed ratio of 1:10. In addition, the highest level of aromatic compound production was equal to 27.3% [(Ref.24)]. In order to improve catalytic performance further, bifunctional and modified catalysts were developed and investigated[25]. Pourkarimi et al. (2022) examined production of bio-oil using two biomasses namely Azolla ferns and Ulva macroalgae, using two catalysts including HZSM-5 zeolite and zeolite-based molybdenum catalyst with catalyst / feed ratio (1:5 and 1:10). They found that the utmost energy efficiency and the lowest amount of pollutants for both Ulva bio-oil and Azolla were determined using Mo/HZSM-5 with catalyst to feed ratio 1:10. Also, the uttermost bio-oil production yield of Azolla and Ulva were obtained using HZSM-5 catalyst and with catalyst / feed ratio equal 1:10[(Ref.26)].

To the best of authors' knowledge, no study has been conducted about using Azolla catalytic pyrolysis and comparing it with Ulva catalytic pyrolysis. Therefore, the present study is a qualitative and quantitative assessment of using catalyst with two biomass including *Azolla filiculoides* and *Ulva fasciata*. Before examining the parameters that affect direct pyrolysis of Azolla and Ulva biomass, they were optimized for the study. The productivity of Azolla and Ulva catalytic pyrolysis using cobalt catalyst based on zeolite with catalyst/feed ratio of 10% was compared with that of direct pyrolysis of the biomasses.

Experimental Section

Preparation of biomass

Anzali Lagoon (North of Iran) was the place of collecting *Azolla filiculoides* biomass. Gulf of Oman was the place of collecting *Ulva Fasciata*. After cleaning the sample (twice using distilled water) and drying under the sunlight for 10 h, the biomasses were ground to obtain a homogenous powder (particle size: 500-1000 μm). The results of elemental and estimate analyses of the two biomasses are provided in our previous work [27].

Preparation of catalysts

Zeolite base used in the study was HZSM-5 zeolite procured from Iran Zeolite with Si/Al ratio of 40. According to the producer, the specific surface of zeolite was 370 m^2/g, with pore size equal to 5.5 and crystallinity equal to 98%. Cobalt metal catalyst was prepared using moist incubation method (Fig. 1). To this end, adequate amounts of the nitrate salts of the metals were mixed with HZSM-5 base solution and then the sample were stirred on a magnetic plate (40 rpm, 25°C, and 4 h) to make sure that the active

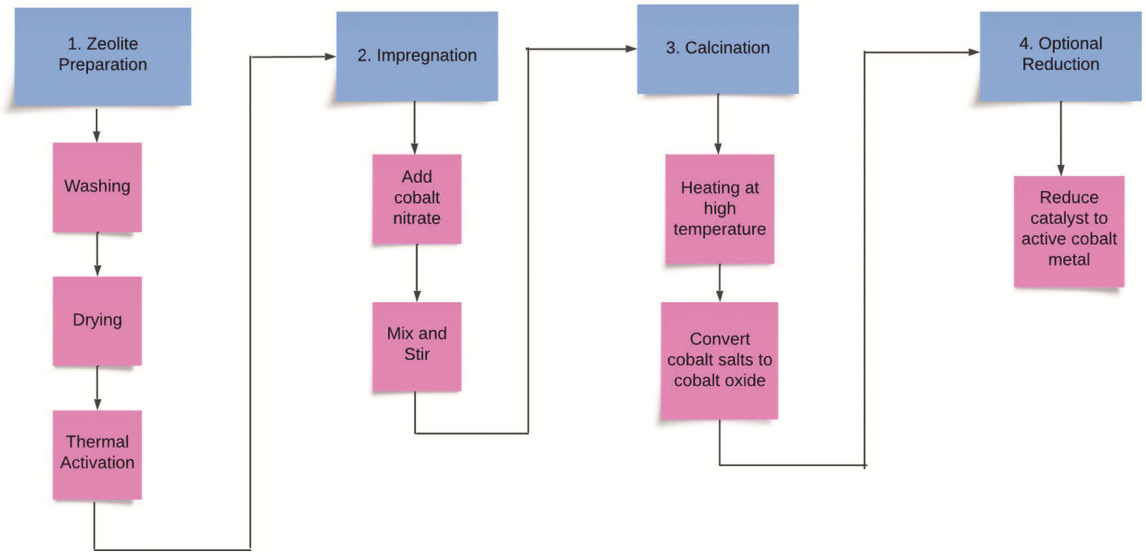

Fig. 1 — Schematic diagram of Co/HZSM-5 catalyst preparation

metal is adsorbed to the base. Afterwards, the samples were dried in an oven (80°C, 18 h) and then calcinated in a furnace with temperature change rate of 3 °C/min at 400°C. The catalyst powder was formed as tablet using a hydraulic press (60 bar) and then grounded with mesh size in 40-60 range (particle size 250-420 µm) for reactor experiments.

Characterisation of catalysts

X-ray light source was Cu Kα with wavelength of 1.54056 Å with 2θ values range from 10 to 90º, which was used to detect crystalline structure of Co/HZSM-5 catalyst. To examine the morphology of synthesized catalysts, SEM analysis was used. Here, FESEM/TESCAN MIRA III (Czech Republic) was used. FTIR/THERMO AVATAR (USA) was used to detect the different functional groups present in the catalyst. BELSORP MINI II (Japan) with vacuum heating up to 450°C was used to do the Brauner-Emmet Teller (BET) analysis.

Experiment device

The experimental setup consisted of three major sections: a reformer, a pyrolysis reactor, and a condenser, as detailed in our previous work[26]. Direct pyrolysis experiments were done using the same setting without the catalyst container of the reformer section[27].

Methodology

The Co/HZSM-5 catalyst with loading ratio of 10% (catalyst/feed ratio 1:10) was used and the experiment was repeated for each biomass. To this end, the catalyst container was prepared beforehand so that a metal mesh with a diameter of 1 cm would be fitted to the longitudinal center of the reformer cylinder and then an asbestos layer was used as coverage. The reformer heater would be set to the optimum temperature[27]. Then, 14 g of biomass would be positioned in the pyrolysis reactor and when the experiment was started, nitrogen carrier (100 mL/min) would be fed to the device for 30 min to remove oxygen of the reactor. The setting including heating rate, temperature, and discharge rate of nitrogen gas would be set according to the findings of our previous study (460°C, carrier gas discharge rate equal to 0.5 L/min, and heating rate equal to 20 °C/min for Azolla experiment; 500°C, carrier gas discharge rate equal to 0.2 L/min, heating rate = 10°C for Ulva experiment)[27]. By achieving the needed temperature, the temperature of reactor would be kept constant for 30 min until the biomass decomposition is completed and secondary reactions are completed while the pyrolysis reactor content passes through the catalyst inside the reformer. Following each experiment, the device was turned off to let it completely cool down and then solid residue (char) is removed from the reactor as biochar. Moreover, the liquid in falcon connected to the condenser is considered as bio-oil. Dichloromethane solvent would be utilized for cleaning the containers and elements of the device. It is notable that all these steps, except for using catalyst were repeated for direct pyrolysis experiments[27].

Having bio-oil and biochar weighed, bio-oil, biochar, and biogas yield were obtained using Eqs (1-3) [28]:

$$\text{Bio-oil yield, wt. \%} = \frac{\text{mass of bio-oil(g)}}{\text{mass of feed}} \times 100 \quad \ldots (1)$$

$$\text{Biochar yield, wt. \%} = \frac{\text{mass of bio-oil(g)}}{\text{mass of feed}} \times 100 \quad \ldots (2)$$

$$\text{Biogas yield. wt. \%} = 100\% - (\text{Bio-oil yield, wt. \%} + \text{Biochar yield, wt. \%}) \quad \ldots (3)$$

Analysis of the obtained bio-oil

To assess the bio-oil samples quality through detecting the compounds, the samples analysis was done using GC-mass 5975C (Agilent Technologies-American company). The qualitative parameters of the obtained fuel using CG-Mass and Biodiesel Analyzer (v.2.2), including iodine number, density, cetane number, and viscosity were determined. To perform elemental analysis, Flash EA1112 was used (Thermo Finnigan- American company) and the results yielded the highest heat value (HHV) using Eq. (4) [10]:

$$HHV\left[\frac{MJ}{kg}\right] = 0.338 * C + 1.428 * \left(H - \frac{O}{8}\right) + 0.095 * S \quad \ldots (4)$$

Where H, C, O, and S refer to hydrogen, carbon, oxygen, and sulfur weight percentage, which were measured using elemental analysis. Using Eqs 4 & 5, energy recovery for the two biomass type were examined[29].

Where $m_{biomass}$ and $m_{bio\text{-}oil}$ are biomass and bio-oil.

$$\text{Energy Recovery (ER)} = \frac{HHV_{biooil} \times m_{biooil}}{HHV_{biomass} \times m_{biomass}} \times 100 \quad \ldots (5)$$

Results and Discussion

XRD analysis

Fig. 2 illustrates XRD results for the catalyst used in the study. The pattern for HZSM-5 zeolite has a sharp peak at 2θ equal to 23.9° and two small peaks of same size at 25.7° and 46°. These peaks indicate the single-phase crystalline structure of the solid. Similar to Co/HZSM-5 catalyst, it appears that the process of metal deposit does not have any effect on the morphology and size of nanoparticles.

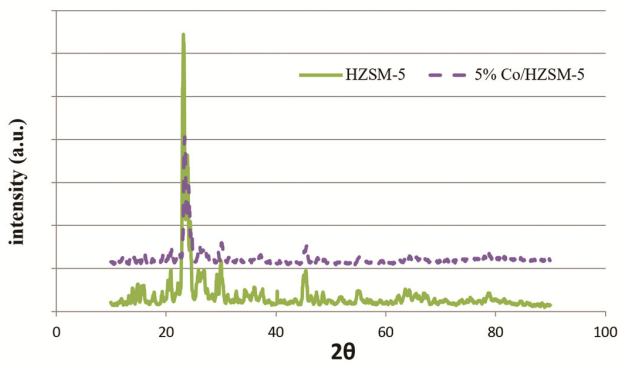

Fig. 2 — XRD analysis of the catalyst used in the study

Pourkarimi et al. (2022) reported sharp peaks in the XRD pattern of HZSM-5 at 2θ = 23.9°, which is characteristic of zeolite HZSM-5. Adding molybdenum nanoparticles did not significantly alter the crystalline structure, consistent with the current study, where cobalt loading also did not affect the HZSM-5 structure[26]. In contrast, Ali et al. (2014) explored the XRD patterns of Co, Ni, and Cu-loaded HZSM-5 catalysts. They found that while the crystalline structure of HZSM-5 was maintained with Ni and Cu, significant structural collapse occurred in the Co/HZSM-5 due to dealumination, forming additional phases like Co_3O_4. This outcome differs from the current study, where no structural collapse was observed, likely due to differences in synthesis methods or conditions[30]. Rostamizadeh et al. (2018) showed that the XRD analysis of Ni-doped HZSM-5 exhibited high crystallinity (97.2%), and that Ni doping did not significantly damage the structure. Similarly, the current findings indicate that cobalt doping did not affect the crystalline structure of HZSM-5. The consistency across these studies suggests that certain metal dopings, like Ni and Co, can preserve the crystalline integrity of HZSM-5[31].

The results of XRD analysis of HZSM-5 zeolite across multiple studies, including our own, consistently show that its crystalline structure is maintained after metal loading (Co, Ni, Cu, Mo), although exceptions have been observed with cobalt under specific conditions. This suggests that while HZSM-5 is generally robust, the effects of metal loading can vary depending on the synthesis conditions and the type of metal used.

SEM analysis

The results of SEM analysis for cobalt catalyst based on zeolite are shown in Fig. 3. Clearly, HZSM-5 catalyst has particles with polyhedron and smooth surface smaller than 5 μm. In addition, as shown for metal catalysts based on zeolite, they have a structure similar to HZSM-5. Apparently, the process of metal deposition does not have a notable effect on the morphology and size of the nanoparticles.

In the study by Pourkarimi et al. (2022), SEM images of HZSM-5 showed smooth polyhedral particles approximately 5 μm in size, indicating a

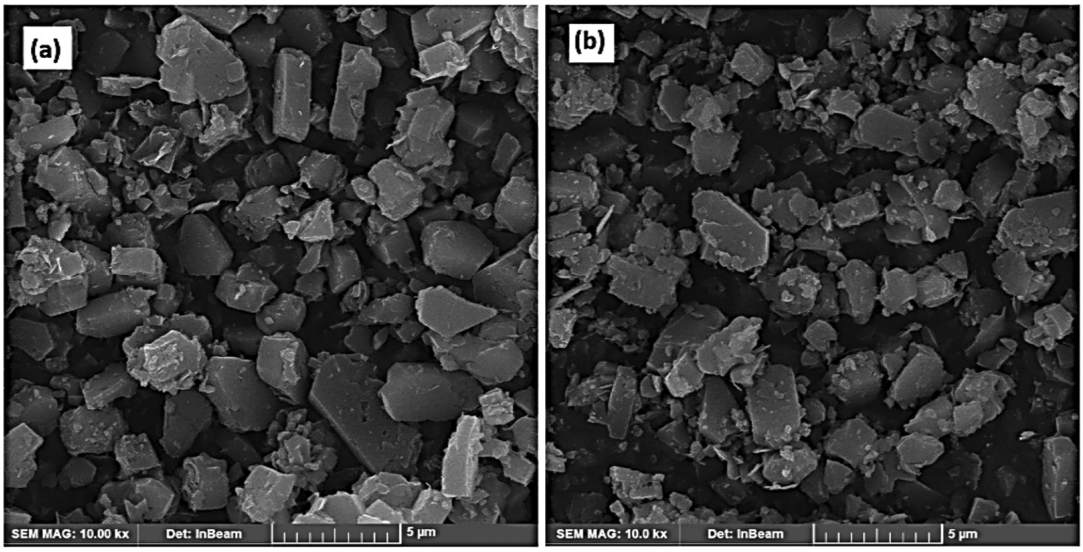

Fig. 3 — SEM catalyst analysis a- HZSM-5 b- Co/HZSM-5

successful synthesis process. The addition of molybdenum nanoparticles did not alter the overall morphology or uniformity of the catalyst. This is consistent with the current study, where cobalt deposition did not affect the general morphology of HZSM-5[26]. Ali et al. (2014) reported that the SEM images of Co, Ni, and Cu-loaded HZSM-5 catalysts exhibited significant differences depending on the metal used. Specifically, for Co/HZSM-5, they observed particle agglomeration and changes in surface roughness, suggesting a potential impact on morphology. This contrasts with the current findings, where cobalt loading did not cause such changes. The discrepancy may be attributed to differences in synthesis methods or conditions[30]. Rostamizadeh et al. (2018) found that Ni-doped HZSM-5 maintained a smooth and uniform morphology, similar to undoped HZSM-5. The SEM images showed no significant changes in particle size or shape after metal doping. This is similar to the current study, cobalt loading did not significantly alter the HZSM-5 structure[31].

The results of SEM analysis across multiple studies suggest that HZSM-5 zeolite generally retains its morphology after metal loading. While some studies, such as that by Ali et al. (2014), observed changes in morphology with cobalt loading, these differences are likely due to variations in synthesis methods and conditions. Overall, the consistency in maintaining particle shape and size across different metal dopings, as seen in this study and others, highlights the robustness of the HZSM-5 structure.

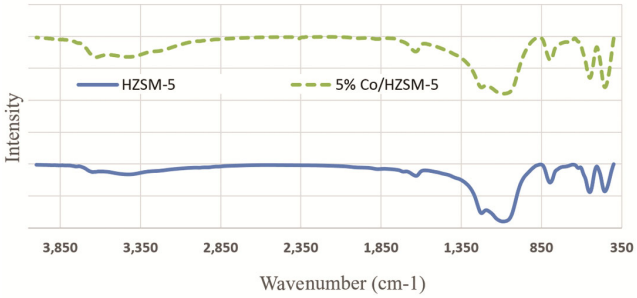

Fig. 4 — FTIR analysis of the catalysis used in the study

FTIR analysis

The FTIR spectrum of HZSM-5 (Fig. 4) features two peaks at 454 cm^{-1} and 548 cm^{-1} which are because of SiO_4 molecular vibration in zeolite. In addition, three peaks are observed at 796, 1089, and 1223 cm^{-1}, which represent strain vibration of Si-O-Al structure. The next peak is at 1640 cm^{-1}, which refers to the vibration bond of water molecules. The last peak is at 3426 cm^{-1}, which refers to O-H bond strain bond caused by the adsorbed water[32]. The FTIR spectrum for metal catalysts based on zeolite (Fig. 4b) is similar to that for HZSM-5 zeolite catalysts. Therefore, adding extra compounds does not cause notable changes in HZSM-5 so zeolite keeps its molecular structure. Similar peaks were observed by our group for Mo-based HZSM-5 catalysts.[26]

Ali et al. (2014) reported similar FTIR spectra for HZSM-5 and metal-loaded zeolite catalysts, with consistent peaks corresponding to the Si-O and Al-O bonds, as well as water absorption. This indicates that the basic structure of the zeolite remains intact after

metal loading[30]. Rostamizadeh et al. (2018) observed that the FTIR spectra of Ni-doped HZSM-5 were also consistent with those of undoped HZSM-5, showing no significant changes in the peaks corresponding to the Si-O-Al framework. This suggests that Ni doping does not disrupt the molecular structure of the zeolite[31]. The results of The FTIR analysis across multiple studies, including the current one, consistently show that the molecular structure of HZSM-5 zeolite is maintained after metal loading. While some minor variations in peak positions may occur depending on the synthesis conditions and metal type, the overall integrity of the Si-O-Al framework is preserved.

BET analysis

BET analysis results for the HZSM-5 and Co/HZSM-5 catalysts are shown in Table 1. As shown in Table 1, the specific surface total pores volume and mean diameter of pores (APD) for the catalyst. As to Co/HZSM-5, the specific surface (SBET) and total pores volume (Vp) are less than those of HZSM-5, and the mean diameter of pores is higher than that of HZSM-5. The reason for this difference is metal nanoparticle residue on the base surface that might block smaller micro-pores on the surface. Moreover, the smaller zeolite pore blockage increases the mean pore size[33]. The ICP analysis was conducted to determine the metal nanoparticle volume on HZSM-5 more accurately compared to the theoretical value (5%) (Table 1). Taking into account the findings, the actual value of cobalt is acceptably near the expected values. Similar results were observed by our group for Mo-based catalysts[26].

Ali et al. (2014) also observed a reduction in surface area and pore volume for metal oxide loaded HZSM-5 catalysts. The study noted that the deposition of metal nanoparticles led to partial pore blockage, similar to the findings reported here[30]. Rostamizadeh et al. (2018) found that Ni-doped HZSM-5 exhibited a slightly reduced surface area compared to the undoped catalyst, with an increase in pore size. This suggests that the deposition of Ni, like cobalt, can result in the partial blockage of smaller pores, leading to changes in pore structure[31].

The result of The BET analysis across multiple studies, including the current one, consistently shows that metal loading on HZSM-5 catalysts typically results in a decrease in surface area and pore volume, accompanied by an increase in average pore diameter. These changes are primarily due to the partial blockage of micropores by metal nanoparticles. While the extent of these changes can vary depending on the synthesis conditions and the type of metal used, the overall trends are consistent across different studies.

Table 1 — BET analysis of the catalyst

Catalysts	S_{BET} (m^2/g)	V_p (Cm^3/g)	APD (nm)	ICP-OES
HZSM-5	329.197	0.059761	3.9659	-
Co/HZSM-5	280.279	0.02492	13.114	4.94

Quantitative assessment of the pyrolysis products

Catalyst pyrolysis experiments and direct pyrolysis of Azolla and Ulva biomasses are listed in Table 2. The highest yields of bio-oil for Ulva and Azolla were 34.43% and 30.64%, respectively, which were obtained from direct pyrolysis process. The primary comparison between bio-oil yield from direct pyrolysis and catalyst pyrolysis indicates that bio-oil yield decreased by 7.17% and 8.03% for Azolla and Ulva, respectively, after adding the catalyst. The decrease in bio-oil yield decreased the yield of biochar yield and increased gaseous products. With the catalyst, the performance of catalytic cracking reactions was improved and with an increase in the light products (gasses) yield, bio-oil and biochar yield decreased. Bio-oil yield of Ulva was higher than that of Azolla both in direct pyrolysis and catalytic pyrolysis. This is also true for biochar yield; while in the case of biogas, Azolla had a better performance than Ulva with direct and catalytic pyrolysis.

Qualitative assessment

Elemental analysis

The outcomes of bio-oil elemental analysis from direct pyrolysis and catalytic pyrolysis experiment, maximum thermal values, and calculated energy performance for Azolla and Ulva are indicated in Table 3 and 4. As shown in Table 3, the HHV for Azolla is 33.2 MJ/kg and the highest energy yield (48.37%) belongs to bio-oil with catalytic pyrolysis. In the case of Ulva, the HHV (32.26 MJ/kg) and the highest energy performance (69.02%) are obtained by catalytic pyrolysis (Table 4).The reason for this can be carbon/oxygen ratio based on elemental analysis; so that the maximum carbon content (69.1% for Azolla and 66.7% for Ulva) and the lowest oxygen content (16.5% for Azolla and 17.3% for Ulva)

Table 2 — Direct and catalytic pyrolysis yield of Azolla and Ulva

Pyrolysis process	Bio-oil %		Bio-char %		Bio-gas %	
	Ulva	Azolla	Ulva	Azolla	Ulva	Azolla
Co/HZSM-5(1:10)	26.1	23.5	43.4	39.5	30.5	37
Direct Pyrolysis	34.43	30.64	49	42.21	16.57	27.14

Table 3 — Bio-oil sample Elemental analysis obtained from Azolla direct and catalytic pyrolysis

Catalysts	C	H	N	O	S	(H/C)*10	O/C	HHV (MJ/kg)	ER (%)
Co/HZSM-5 (1:10)	69.1	8.95	5.31	16.5	0.14	1.3	0.24	33.2	48.37
Direct Pyrolysis	51.23	6.87	4.21	37.58	0.11	1.34	0.73	20.43	36.8

Table 4 — Bio-oil sample elemental analysis obtained from Ulva direct and catalytic pyrolysis

Catalysts	C	H	N	O	S	(H/C)*10	O/C	HHV (MJ/kg)	ER (%)
Co/HZSM-5 (1:10)	66.7	8.8	4.7	17.3	2.5	1.32	0.26	32.26	69.02
Direct Pyrolysis	49.25	6.65	3.25	38.7	2.15	1.35	0.79	19.44	54.6

were observed in bio-oil samples obtained through catalytic pyrolysis. The carbon content increase and oxygen content decrease can increase HHV. This shows that while production performance of bio-oil for Ulva and Azolla decreases with catalyst, there is considerable growth in HHV and energy yield of the fuel. In addition, a comparison of Azolla and Ulva elemental analysis indicates that HHV of Azolla in both direct pyrolysis and catalytic pyrolysis exceeded that of Ulva. On the other hand, the energy yield of Ulva was higher compared to Azolla because of a higher bio-oil yield.

Among the advantages of catalytic pyrolysis, the H/C ratio increase, and O/C ratio decrease in bio-oil yield can increase heat value and energy yield of the fuel. Vankrolen (2007) introduced a diagram to compare optimum performance of different fuels based on H/C and O/C ratio in fuels. Fig. 5 illustrates Vankrolen's diagram[34]. The areas marked on the diagram indicate the optimum H/C and O/C ratios for different types of fuels for which the HHV and energy yield are obtained. The optimum range determined for H/C pyrolysis oil is in 1.3-1.6 range and for O/C it is in 0.2-0.4 range. The H to C and O to C percentages for the bio-oil obtained from direct pyrolysis and catalytic pyrolysis of biomasses are listed in Table 3 and 4. As shown, the H/C ratio for bio-oil samples (1.3-1.35) is in the optimum range of Vankrolen diagram; while in the case of O/C ratio, the direct pyrolysis O/C ratio is in 0.7-0.8 range, which is beyond the optimum range in Vankrolen's diagram. In the case of bio-oil generated through catalytic pyrolysis, this range is 0.2-0.3, which is the optimum range. Therefore, the bio-oil generated through catalytic pyrolysis of bio-oil has an optimum performance in terms of Vankrolen's diagram, while the bio-oil of direct pyrolysis does not have an optimum performance because of O/C ratio.

Combinational analysis

The qualitative characteristics of biomass samples obtained from direct pyrolysis and catalytic pyrolysis can be studied through GC-MS analysis.

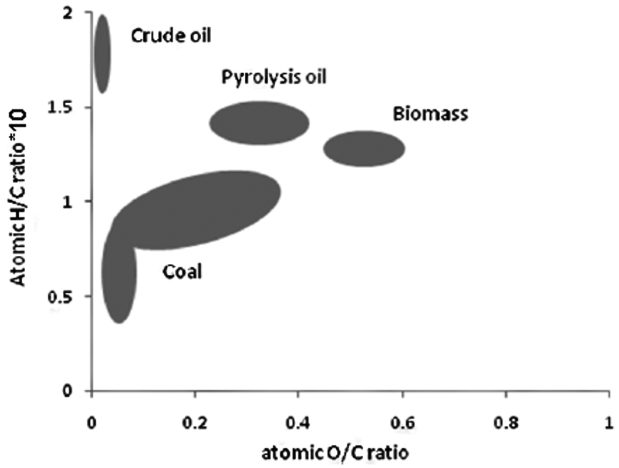

Fig. 5 — Vankrolen diagram

The GC-MS analysis results for the samples are given in Table 5.

Given the results of GC-MS analysis, the key compound groups in bio-oil samples including aromatic compounds, nitrogenated compounds, oxygenated compounds, alkanes/alkenes, and phenolic compounds and the specific values for Azolla and Ulva are illustrated in Fig. 6. Using the catalyst, alkene / alkane content was decreased, while the decrease for Ulva was notably higher than that of Azolla. While the higher content of alkane / alkene can increase heat value of fuel, to some extent, presence of more efficient compounds like aromatics and oxygenated compounds overshadow their effect. Aromatic compound content increased notably in the two biomasses due to using catalysts, which increased the HHV in comparison to the bio-oil collected from direct pyrolysis. It is notable that using catalysts can cause more complicated reactions and increase aromatic products' yield. As to oxygenated compounds, catalytic pyrolysis decreased oxygenate compound ratio in a notable way with a positive impact on thermal value of the fuel and burning quality. This positive impact is stronger in Ulva compared to Azolla. In addition, catalytic pyrolysis increased and decreased nitrogenated compounds content for Ulva Azolla bio-oils, respectively. Therefore,

Table 5 — GC-MS analysis results of the bio-oil samples from direct pyrolysis and catalytic pyrolysis

Row	Component	Formula	Co/HZSM-5 (1:10)		Direct Pyrolysis	
			Ulva	Azolla	Ulva	Azolla
1	Phenol	C_6H_6O	1.1	5.3	2.7	15.5
2	4-ethyl-phenol	$C_8H_{10}O$	1.05	0.62	-	3.1
3	2-methyl-phenol	C_7H_8O	1.73	1.63	-	4.4
4	Para-Crousol	C_7H_8O	4.75	4.63	-	11.2
5	2-5-dimethyl-phenol	$C_8H_{10}O$	0.78	0.76	-	1.6
6	4-methyl-phenol	C_7H_8O	1.97	1.52	-	-
7	Catechol	$C_6H_6O_2$	3.05	3.21	-	9.2
8	Toluene	C_7H_8	8.3	8.00	3.25	3.1
9	Benzene	C_6H_6	4.3	4.47	2.8	-
10	Styrene	C_8H_8	2.5	2.42	3.3	-
11	Ethyl benzene	C_8H_{10}	4.0	4.18	-	2
12	2-Methyl-naphtalen	$C_{11}H_{10}$	3.3	2.86	-	1.3
13	Prydine	C_5H_5N	1.3	1.78	-	1.6
14	Indole	C_8H_7N	5.7	7.85	0.8	7.6
15	3-methyl-prydine	C_6H_7N	1.5	1.97	-	1.6
16	3-prydinol	C_5H_5NO	2.1	2.79	-	2.6
17	Hexadecane	$C_{16}H_{34}$	1.55	1.28	-	1.6
18	Heptadecane	$C_{17}H_{36}$	1.65	1.36	-	-
19	Pentadecane	$C_{15}H_{32}$	1.7	1.48	-	-
20	Limonene	$C_{10}H_{16}$	1.7	1.58	-	-
21	2-Foran-Methanol	$C_5H_6O_2$	2.9	2.78	-	2.3
22	Piroul	C_4H_5N	2.2	3.7	-	-
23	Cyclo-pentan	C_5H_{10}	1.95	2.05	-	-
24	Bis-phetalat	$C_{24}H_{38}O_4$	3.5	3.25	-	-
25	3-methyl, 3-cyclopentenedione	$C_6H_6O_2$	1.05	0.84	-	1.5
26	Hexadecanal	$C_{16}H_{32}O$	1.75	1.35	3.2	-
27	Undecane nitril	$C_{11}H_{21}N$	0.95	1.26	1.1	-
28	Ethyl-acetate	$C_4H_8O_2$	1.35	0.98	11.9	-
29	Allyl Nonanoate	$C_{12}H_{22}O_2$	1.15	0.84	2.8	-
30	3-Dodecene	$C_{12}H_{24}$	1.3	1.25	1	-
31	3-methyl-2-cycloPentene	C_6H_{10}	-	-	-	0.8
32	1-Ethyl-3-methylbenzene	C_9H_{12}	-	-	-	1.75
33	1,2,3-trimethylbenzene	C_9H_{12}	-	-	-	1.2
34	2,3-Dimethy1-3-cycloPentene	C_7H_{12}	-	-	-	0.7
35	2-Methoxyphenol	$C_7H_8O_2$	-	-	-	0.7
36	2-Ethyl phenol	$C_8H_{10}O$	-	-	-	1
37	2,4-Dimethyl phenol	$C_8H_{10}O$	-	-	-	2.7
38	3,5-Dimethyl phenol	$C_8H_{10}O$	-	-	-	2
39	2-Ethyl benzimidazole	$C_9H_{10}N_2$	-	-	-	1.7
40	4-Methyl-1, 2-benzenediol	$C_7H_8O_2$	-	-	-	4.42
41	1-Tridecene	$C_{13}H_{26}$	-	-	-	1.1
42	2-Tetradecene	$C_{14}H_{28}$	-	-	7.2	1.6
43	Bis(2-ethylhexyl) phthalate	$C_{24}H_{38}O_4$	-	-	-	1
44	Nanodecane	$C_{19}H_{40}$	-	-	-	1.5
45	2-Ethynyl pyridine	C_7H_5N	-	-	3.7	-
46	1H-Pyrrole	C_4H_4N	-	-	9.9	-
47	2-Butene-1,4-diol	$C_4H_8O_2$	-	-	5.8	-
48	2-Methylene-4-pentenal	C_6H_8O	-	-	2.3	-
49	1H-Pyrrole, 3-methyl	C_5H_7N	-	-	3.2	-
50	Phenol,4-methylene	C_7H_8O	-	-	5.8	-
51	1-Octanol,3, 7-dimethyl	$C_{10}H_{22}O$	-	-	0.9	-
52	2,5-Dimethyl-4-hydroxy-3(2H)-furanone	$C_6H_8O_3$	-	-	2.4	-
53	1H-Indene, 1-methylene	$C_{10}H_8$	-	-	3.2	-
54	Benzonitrile, 3-methyl	C_8H_7N	-	-	1.1	-
55	Nonane,2,6-dimethyl	$C_{11}H_{24}$	-	-	0.8	-
56	2-methyl-3-butenyl	C_5H_9O	-	-	2.5	-
57	Nonan-4-one	$C_9H_{18}O$	-	-	2.5	-
58	Indolizine	C_8H_7N	-	-	3.2	-
59	E-2-Tetradecen-1-ol	$C_{14}H_{28}O$	-	-	5.6	-
60	1-Tridecyne	$C_{13}H_{24}$	-	-	1.3	-
61	Decanoic Acid	$C_{10}H_{20}O_2$	-	-	1.1	-
62	Tetradecanamide	$C_{14}H_{29}NO$	-	-	3.8	-
63	2-Undecene, 3-methyl	$C_{12}H_{24}$	-	-	1.3	-

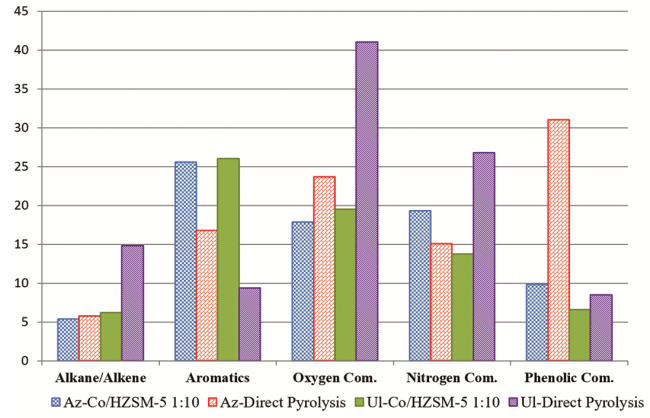

Fig. 6 — Key compound groups in Ulva and Azolla bio-oil sample of Ulva and Azolla through direct and catalytic pyrolysis

contamination caused by Azolla bio-oil is less than that of caused by Ulva bio-oil. The reason for this is the difference in protein content in Azolla and Ulva biomasses. Azolla biomass (18.34%) has higher protein content than Ulva (15.9%). In the case of

Table 6 — Qualitative parameters of the bio-oil samples and standard range

Quality parameter	Direct Pyrolysis		Co/HZSM-5 1:10		Standard EN14214
	Azolla	Ulva	Azolla	Ulva	
Cetan number (CN)	67.1	62.4	71.4	69.8	51<
Iodine value (IV) g/100g oil	130	125	116	116.3	120>
Density (g/cm^3)	0.91	0.84	0.89	0.86	0.86-0.9
Kinematic viscosity (mm^2/s)	4.3	3.9	4.35	4.41	3.5-5
Cloud point (°C)	-3.3	-3.5	4.28-	4.35-	-

Azolla, the protein content is decomposed by catalytic pyrolysis so that nitrogenated compounds content in Azolla bio-oil is higher. In the case of Ulva, however, the decomposed hydrogen compounds are converted into gas products, so that nitrogenated compounds content is lower in Ulva bio-oil obtained through catalytic pyrolysis compared to direct pyrolysis[35]. Eventually, using the catalyst decreased phenolic compounds notably in Azolla and to some extent in Ulva. The increase in aromatic compounds due to the use of catalyst increases heat value of fuel, while it also increases the pollution caused by the burning the fuel when the increase in heat value is more than 25% [36]. In the case of the catalyst used in this study, aromatic content in Azolla bio-oil was 25.56% and 26.05% in Ulva bio-oil. Therefore, the catalyst trivially affected the pollutants caused by burning the fuel. On the other hand, phenolic compound decreased notably due to the use of catalyst, which indicates a decrease in pollution load of bio-oil obtained from catalytic pyrolysis compared to the bio-oil obtained through direct pyrolysis.

Some of the qualitative specifications of the produced fuels including iodine number, cetane number, cinematic viscosity, density, and cloud point were determined using GC-Mass analysis results in Biodiesel Analyzer v.2.2. Table 6 indicates the qualitative parameters of the produced bio-oil and the standard values (EN14214-2012) [10]. With the catalyst, cetane number of Azolla and Ulva bio-oils increased by 6.4% and 11.8% respectively and iodine number decreased by 10.8% and 7%, respectively, which improved performance quality of the fuels. In addition, density and viscosity of the biofuels did not change notably after using the catalyst. However, the cloud point decreased to some extent, which makes the fuels suitable for lower temperatures. Using the catalyst had a positive impact on the quality of fuel (cetane and iodine numbers in particular) and the application range.

Conclusion

This study compared the impacts of cobalt-based zeolite catalyst with direct pyrolysis on two biomasses, Azolla and Ulva. While catalytic pyrolysis reduced bio-oil yields (23.5% for Ulva, 26.1% for Azolla), it essentially upgraded the heat value (32.26 MJ/kg for Ulva, 32.2 MJ/kg for Azolla) by increasing carbon content and reducing oxygen content. The bio-oil produced through catalytic pyrolysis met the optimal standards for pyrolysis oil, with improved cetane and iodine numbers, indicating higher quality. Although the catalyst had minimal impact on density and viscosity, it effectively increased energy performance. Ulva bio-oil exhibited higher yield and energy efficiency with lower pollutants, whereas Azolla offered superior heat value and cetane number. Thus, catalytic pyrolysis is a promising method for producing high-quality bio-oil.

References

1 Vuppaladadiyam A K, Vuppaladadiyam S S V, Sahoo A, Murugavelh S, Anthony E, Bhaskar T, Zheng Y, Zhao M, Duan H, Zhao Y, Antunes E, Sarmah A K & Leu S Y, Bio-oil and biochar from the pyrolytic conversion of biomass: A current and future perspective on the trade-off between economic, environmental, and technical indicators, *Sci Total Environ*, 857 (2023) 159155.

2 Marques J de A O, Alves J L F, de Oliveira G P, Melo D M de A, de Melo Viana G A C & Braga R M, Catalytic flash pyrolysis of Scenedesmus sp. post-extraction residue using low-cost HZSM-5 catalyst with the perspective to produce renewable aromatic hydrocarbons, *Environ Sci Pollut Res*, 31 (2024) 18785.

3 Ayub H M U, Ahmed A, Lam S S, Lee J, Show P L & Park Y K, Sustainable valorization of algae biomass via thermochemical processing route: An overview, *Bioresour Technol*, 344 (2022) 126399.

4 Quevedo-Amador R A, Escalera-Velasco B P, Arias A M R, Reynel-Ávila H E, Moreno-Piraján J C, Giraldo L & Bonilla-Petriciolet A, Application of waste biomass for the production of biofuels and catalysts: a review, *Clean Technol Environ Policy*, 26 (2024) 943.

5 Pourkarimi S, Hallajisani A, Nouralishahi A, Alizadehdakhel A & Golzary A, Factors affecting production of beta-carotene from dunaliella salina microalgae, *Biocatal Agric Biotechnol*, 29 (2020) 101771.

6 Sun J, Norouzi O & Mašek O, A state-of-the-art review on algae pyrolysis for bioenergy and biochar production, *Bioresour Technol*, 346 (2021) 126258.

7 Jalilian N, Najafpour G D & Khajouei M, Macro and micro algae in pollution control and biofuel production-A review, *Chem Bio Eng Rev*, 7 (2020) 18.

8 Miao X, Wu Q & Yang C, Fast pyrolysis of microalgae to produce renewable fuels, *J Anal Appl Pyrol*, 71 (2004) 855.

9 Grierson S, Strezov V & Bengtsson J, Life cycle assessment of a microalgae biomass cultivation, bio-oil extraction and pyrolysis processing regime, *Algal Res J*, 2 (2013) 299.

10 Pourkarimi S, Hallajisani A, Alizadehdakhel A & Nouralishahi A, Biofuel production through micro-and macroalgae pyrolysis-A review of pyrolysis methods and process parameters, *J Anal Appl Pyrol*, 142 (2019) 104599.

11 Sekar M, Mathimani T, Alagumalai A, Chi N T L, Duc P A, Bhatia S K, Brindhadevi K & Pugazhendhi A, A review on the pyrolysis of algal biomass for biochar and bio-oil-Bottlenecks and scope, *Fuel*, 283 (2021) 119190.

12 Gökdai Z, Sinaug A & Yumak T, Comparison of the catalytic efficiency of synthesized nano tin oxide particles and various catalysts for the pyrolysis of hazelnut shell, *Biomass Bioenergy*, 34 (2010) 402.

13 Perego C & Bosetti A, Biomass to fuels: The role of zeolite and mesoporous materials, *Micropor Mesopor Mater*, 144 (2011) 28.

14 Ferreira A F, Dias A P S, Silva C M & Costa M, Bio-oil and bio-char characterization from microalgal biomass, *MEFTE*, 11 (2014) 99.

15 Mohamed A R, Hamzah Z, Daud M Z M & Zakaria Z, The effects of holding time and the sweeping nitrogen gas flowrates on the pyrolysis of EFB using a fixed bed reactor, *Procedia Eng*, 53 (2013) 185.

16 Mohamed A R & Hamzah Z, An alternative approach for the screening of catalytic empty fruit bunch (EFB) pyrolysis using the values of activation energy from a thermogravimetric study, *React Kinet Mech Catal*, 114 (2015) 529.

17 Li L, Rowbotham J S, Greenwell C H & Dyer P W, An introduction to pyrolysis and catalytic pyrolysis: Versatile techniques for biomass conversion, *Catal Biomass Convers*, (2013) 173.

18 Jones S B, Valkenburt C, Walton C W, Elliot D C, Holladay J E, Stevens D J, Kinchin C & Czernik S, Production of Gasoline and Diesel from Biomass via Fast Pyrolysis, Hydrotreating and Hydrocracking: A Design Case, *U S Dept Energy*, 2009.

19 Naqvi S R, Khoja A H, Ali I, Naqvi M, Noor T, Ahmad A, Luque R & Amin N A S, Recent progress in catalytic deoxygenation of biomass pyrolysis oil using microporous zeolites for green fuels production, *Fuel*, 333 (2023) 126268.

20 Amalina F, Krishnan S, Zularisam A W & Nasrullah M, Effect of process parameters on bio-oil yield from lignocellulosic biomass through microwave-assisted pyrolysis technology for sustainable energy resources: Current status, *J Anal Appl Pyrol*, 171 (2023) 105958.

21 Pan P, Hu C, Yang W, Li Y, Dong L, Zhu L, Tong D, Qing R & Fan Y, The direct pyrolysis and catalytic pyrolysis of Nannochloropsis sp. residue for renewable bio-oils, *Bioresour Technol*, 101 (2010) 4593.

22 Mohammed I Y, Abakr Y A, Yusup S & Kazi F K, Valorization of Napier grass via intermediate pyrolysis: Optimization using response surface methodology and pyrolysis products characterization, *J Clean Prod*, 142 (2017) 1848.

23 Ma C, Geng J, Zhang D & Ning X, Non-catalytic and catalytic pyrolysis of Ulva prolifera macroalgae for production of quality bio-oil, *J Energy Inst*, 93 (2020) 303.

24 Chen W H, Cheng C L, Lee K T, Lam S S, Ong H C, Ok Y S, Saeidi S, Sharma A K & Hsieh T H, Catalytic level identification of ZSM-5 on biomass pyrolysis and aromatic hydrocarbon formation, *Chemosphere*, 271 (2021) 129510.

25 Yap T L, Loy A C M, Chin B L F, Yau L J, Alhazmi H, Chai Y H, Yiin C L, Cheah K W, Wee M X J, Lam M K, Jawab Z A, Yusup S & Lock S S M, Synergistic effects of catalytic co-pyrolysis Chlorella vulgaris and polyethylene mixtures using artificial neuron network: Thermodynamic and empirical kinetic analyses, *J Environ Chem Eng*, 10 (2022) 107391.

26 Pourkarimi S, Sadeh M S, Hallajisani A, Hajikhani M, Moradi M, Alizadeh O & Nouralishahi A, Investigation of catalytic pyrolysis of Azolla filiculoides and Ulva fasciata for bio-oil production, *Biochem Eng J*, 178 (2022) 108278.

27 Pourkarimi S, Hallajisani A, Alizadehdakhel A & Nouralishahi A, Bio-oil production by pyrolysis of Azolla filiculoides and Ulva fasciata macroalgae, *Glob J Environ Sci Manag*, 7 (2021) 331.

28 Brennan L & Owende P, Biofuels from microalgae-a review of technologies for production, processing, and extractions of biofuels and co-products, *Renew Sustain Energy Rev*, 14 (2010) 557.

29 Song L, Hu M, Liu D, Zhang D & Jiang C, Thermal cracking of Enteromorpha prolifera with solvents to bio-oil, *Energy Convers Manag*, 77 (2014) 7.

30 Ali I O, El-Molla S A, Ibraheem I A & Salama T M, Synthesis and characterization of metal oxides loaded-HZSM-5 and their implication for selective conversion of isopropanol, *Micropor Mesopor Mater*, 197 (2014) 48.

31 Rostamizadeh M, Yaripour F & Hazrati H, Ni-doped high silica HZSM-5 zeolite (Si/Al = 200) nanocatalyst for the selective production of olefins from methanol, *J Anal Appl Pyrol*, 132 (2018) 1.

32 Shen L & Zhang D K, An experimental study of oil recovery from sewage sludge by low-temperature pyrolysis in a fluidised-bed, *Fuel*, 82 (2003) 465.

33 Ren X Y, Cao J P, Zhao X Y, Yang Z, Liu S N & Wei X Y, Enhancement of aromatic products from catalytic fast pyrolysis of lignite over hierarchical HZSM-5 by piperidine-assisted desilication, *ACS Sustain Chem Eng*, 6 (2018) 1792.

34 Ben H, Wu F, Wu Z, Han G, Jiang W & Ragauskas A J, A comprehensive characterization of pyrolysis oil from softwood barks, *Polymers*, 11 (2019) 1387.

35 Li H, Wang Y, Zhou N, Dai L, Deng W, Liu C, Cheng Y, Liu Y, Cobb K, Chen P & Ruan R, Applications of calcium oxide–based catalysts in biomass pyrolysis/gasification -A review, *J Clean Prod*, 291 (2021) 125826.

36 Sun Y, Gao B, Yao Y, Fang J, Zhang M, Zhou Y, Chen H & Yang L, Effects of feedstock type, production method, and pyrolysis temperature on biochar and hydrochar properties, *Chem Eng J*, 240 (2014) 574.